

## Bubble Creation in Water with Dissolved Gas: Prediction of Regions Endangered by Cavitation Erosion

Patrik Zima<sup>1\*</sup>, Milan Sedlár<sup>2</sup>, František Maršík<sup>1</sup>

<sup>1</sup>Department of Thermodynamics, Institute of Thermomechanics,  
Academy of Sciences of CR, Dolejškova 5, 18200, Prague, Czech Republic

<sup>2</sup>Sigma Research and Development Institute, J. Sigmunda 79, 78350 Lutín, Czech Republic

\*E-mail: zimap@it.cas.cz

The regions on the blades of the mixed-flow pump impeller which are endangered by cavitating bubbles are determined numerically. The regions are then compared with the real water pump damaged by cavitation erosion after a long operation. The viscous flow analysis is based on solving 3D Reynolds-averaged Navier-Stokes equations with turbulence modeling. The Rayleigh-Plesset equation is integrated along the trajectories for the given initial bubble size distribution. Simple quantities are introduced as a measure of the mechanical action of the bubble interface on the surrounding liquid. This action is then evaluated along the streamlines nearest to the blade surface and compared with the real picture of erosion. The article also summarizes the key points of the extended classical theory of homogenous nucleation designed to predict the bubble nucleation rates in real aqueous systems. The theory assumes that non-equilibrium effects involved in the nucleus formation lower the nucleation barrier predicted by the classical theory for the case of cavitation.

### 1. Introduction

One of the fundamental and intriguing properties of ordinary water is its tendency to entrap, dissolve and release air to form cavitating bubbles when subjected to a sudden decrease of pressure [1] (even at pressures considerably higher than the equilibrium vapor pressure). This process occurs in a number of industrial applications. The authors'



Fig. 1. Erosion of the blades of the mixed-flow pump impeller of Sigma Lutín, the largest Czech manufacturer of water pumps.

main concern is the critical importance of this process in pump design. The presence of cavitating bubbles often determines the design parameters of the pump as a result of cavitation erosion, vibration and reduced efficiency. In Fig. 1, we show a photograph of erosion of the cast-iron blades of a mixed-flow pump impeller.

One of the preconditions for successful modeling of the effects of cavitation is the ability to predict the occurrence/rate of creation of bubbles. In order to study the problem theoretically one has to see water as a solution of water and gas with other chemical and mechanical contents. One of the objectives of this research of cavitation in the real aqueous systems is to determine the actual number, critical (or initial) size and composition of the microscopic bubble sites and to relate these quantities to the chemical and mechanical composition, temperature and even the history of treatment (i.e. usually the pressure history) of the aqueous system using thermodynamically consistent tools. Since this is by no means an easy challenge it is not surprising that in our present ability and knowledge we are often content with models based on empirical estimations of the number and size distribution of pre-existing microscopic bubbles in the flow of water.

## 2. Extension of the Classical Theory of Homogeneous Nucleation

This section briefly summarizes the fundamentals of the theoretical extension of the classical theory of homogeneous nucleation. This has been made in order to determine the number and size of bubble nuclei in real liquid mixtures. The theory presented in [2] takes into account the real properties of fluids (liquid mixtures) and assumes that non-equilibrium effects associated with irreversible processes involved in the nucleus formation are responsible for changing the nucleation barrier predicted by the classical theory. These effects can increase the nucleation work for condensation and decrease the nucleation work for cavitation and boiling. The generalization of the theory for the case of bubble nucleation has been presented in Ref. [3], where some experimental and numerical results are included and the principle of thermodynamic fluctuations is utilized to determine the equilibrium bubble nucleation work.

The effect of non-equilibrium (dissipative) processes (e.g. inertial and damping forces coupled with evaporation and diffusion of contaminant gas) on the work of formation of a nucleus of the new phase is expressed using a substance-dependent correction coefficient  $\alpha$  which must be determined experimentally. The nucleation work  $W$  is split into the equilibrium portion  $W_{eq}$  and the non-equilibrium portion  $F_{noneq}$ :

$$W = W_{eq} + F_{noneq} = W_{eq}(1 - 2\alpha),$$

$$\text{i.e. } \alpha = -\frac{F_{noneq}}{2W_{eq}}, \text{ where } 0 \leq \alpha \leq 1/2. \quad (1)$$

In order to obtain the equilibrium portion of the nucleation work  $W_{eq}$  for cavitation the theory of thermodynamic fluctuations is applied [3] yielding:

$$W_{eq} = \sigma k T \left( -\frac{4\pi}{3(kT)^2 (\partial p / \partial V)_T} \right)^{1/3}. \quad (2)$$

where  $\sigma$  is surface tension,  $k$  is the Boltzmann constant,  $T$  is temperature,  $p$  is pressure and  $V$  is volume. The value of  $\alpha$  has been estimated for tap water based on the assumed value of the nucleation rate  $J = 10^{12}$  nuclei  $m^{-3} s^{-1}$  from the preliminary experiments described in [3]. The resulting value  $\alpha = 0.4994$  corresponds to the non-equilibrium portion of the nucleation work being equal in

magnitude to the equilibrium portion of the work and the critical radius  $R = 6.5 \times 10^{-7}$  m. The value of  $\alpha$  has an insignificant dependence on the assumed value of  $J$  for critical radii roughly  $R > 10^{-8}$  m.

The nucleation rates predicted by the revised theory are very high indicating that substantial non-equilibrium effects are responsible for lowering the nucleation rates. The energy dissipation during bubble formation must be studied further. Possible areas for investigation are the effect of temperature fluctuations and the dependence of surface tension on curvature and chemical composition.

## 3. Numerical Modeling of Cavitation in a Radial Pump

**3.1. Motivations** The adverse effects of cavitation in hydromachinery are reduced performance, flow instabilities, vibrations, noise, and material erosion. The main contribution to erosion of material arises from the mechanical effects of the violent collapse of bubbles near the solid surface. These effects can be represented by the impact of a spherical shock wave propagated from the center of the collapsing bubble or by a jet produced during an asymmetric bubble collapse. These two mechanisms act on the solid surface either directly (erosion) or indirectly (fatigue due to plastic deformations of the surface).

In this work we will restrict ourselves to detection of surfaces which are most endangered with direct mechanical erosion while any chemical effects (such as corrosion) will be neglected.

**3.2. 3D model** The viscous flow analysis is based on 3D Reynolds-averaged Navier-Stokes

s. The turbulence is modeled using the high Reynolds number  $k$ - $\epsilon$  model ( $k$  is the specific turbulent kinetic energy and  $\epsilon$  is turbulent kinetic energy dissipation rate). The finite element method with penalization and reduced integration is applied, based on the linear hexahedron. The upwinding method uses artificial viscosity operator constructed to operate in the flow direction only and to eliminate any crosswind artificial diffusion [4]. A generalized form of the penalty formulation is used to take into account the density change in the bubbly regions.

**3.3. Bubble dynamics model** At our current level of knowledge based on only limited experimental data we are unable to relate the theory presented in the previous section to the number of bubble nuclei in the flow. Instead, we assume a finite number of bubble sizes with initial radius  $R_{0i}$  and nuclei

number  $\eta_i$  in the unit volume with the density calculated as follows [5]:

$$\rho = \rho_l(1 - \eta_i \tau_i), \quad \tau_i = 4\pi R_{0i}^3 / 3. \quad (3)$$

No bubble interaction is considered. The local radius of each bubble is obtained as the solution to the Rayleigh-Plesset equation:

$$\begin{aligned} R\ddot{R} + \frac{3}{2}\dot{R}^2 + \frac{4v_e\dot{R}}{R} + \frac{2\sigma}{\rho_l R} \left( 1 - \left( \frac{R_0}{R} \right)^{3\kappa-1} \right) &= \\ = \frac{p_v - p_0}{\rho_l} \left( 1 - \left( \frac{R_0}{R} \right)^{3\kappa} \right) + \frac{p_0 - p}{\rho_l} + & \\ + \frac{R}{\rho_l c_l} \frac{D}{Dt} (p_g - p). \end{aligned} \quad (4)$$

In the above equation,  $p_0$  is the liquid ambient pressure at undisturbed initial condition,  $p_v$  is the equilibrium vapor pressure,  $p_g$  is the gas pressure in the bubble,  $\rho_l$  is liquid density,  $c_l$  is the sound velocity of the liquid,  $\sigma$  is the surface tension of the liquid and  $\kappa$  is the polytropic index of the non-condensable gas mixture in the bubble. The effective viscosity  $v_e$  has been chosen between  $v_e = v_l$  and  $10v_l$  to ensure satisfactory numerical damping.

Equation (4) is integrated along the flow characteristics using the fourth-order Runge-Kutta scheme [5] which enables to alter the time step during the calculation. The adaptive step-size algorithm is employed to ensure sufficiently small time steps for marching through violent bubble collapses [6], especially the first ones.

In order to obtain the bubble size distribution for each grid point of the mesh, the backward trajectory going through the grid point is calculated and the Rayleigh-Plesset equation is integrated along the trajectory for different initial bubble sizes. The resulting density distribution is used to reiterate the continuity and momentum equations. When the iteration process is finished, the erosion driving forces  $EF_1$  and  $EF_2$  are evaluated along the streamlines going through the grid points nearest to the blade surface:

$$EF_1 = \sum_i F_{1i} N_i, \quad EF_2 = \sum_i F_{2i} N_i \quad (5)$$

where  $N_i$  is the number of events corresponding to the bubble size  $i$  per second and square meter.  $F_1$  and  $F_2$  are inertial forces defined as follows:

$$\begin{aligned} F_1 &= (4/3)\pi\rho_l\dot{R}R^3, \\ F_2 &= 4\pi\rho_l(R\dot{R})^2. \end{aligned} \quad (6)$$

As will be shown in the results the two forces are unsophisticated measures of the mechanical erosion of the blade surface. They represent the action of the bubble interface on the surrounding liquid. An unknown part of the energy emitted during the bubble interface motion is responsible for the erosion. Using the forces defined in Eq. (5) we will now attempt to relate the aggregate energy emitted during the bubble motion to the final picture of mechanical erosion on the blade surface after a number of operating cycles of the pump.

**3.4. Test case** In the present study, the flow past the blades of a mixed-flow pump impeller shown in Fig. 2 is considered. The H-type structured grid (about 80,000 nodes) with a simple I-grid for the treatment of the blade trailing edge cut-off represents only one blade-to-blade passage. The flow rate is 0.78 of the optimum one, the inlet pressure is 75 kPa. In the process of bubble dynamics calculation, all water properties are defined at 20°C. The initial bubble size distribution has been predefined according to the measurements by Waniewski et al [7]. The total number of nuclei corresponds to the initial void fraction  $\alpha_0 = 0.002\%$ . We assume ten nuclei sizes ranging from 10 to 200  $\mu\text{m}$ .

**3.5. Results and discussion** Figures 3 and 4 show the results of the numerical simulation projected on the photographs of the eroded pump blade. The contour A in Fig. 3 delimits the region of the first (strongest) collapses of the cavitation bubbles. The hatched area B (sub-area of A) is characterized by the value  $\log_{10}|EF_1| > 6$ . It can be seen that this area roughly corresponds to the hole in the blade. The solid line in Fig. 4 delimits the area characterized by the value  $\log_{10}|EF_1| > 3$  and the line with squares represents the value  $\log_{10}|EF_1| = 4$  upstream of the first collapses. The values of the forces  $EF_2$  are not plotted because they are almost identical to the values of  $EF_1$ .

The first collapse of the bubble evidently plays a major role in the cavitation erosion. The magnitude of the force is enhanced for bubbles with large time scales of growth (undergoing slow pressure changes). Such bubbles have enough time to grow many more times its initial radius and consequently

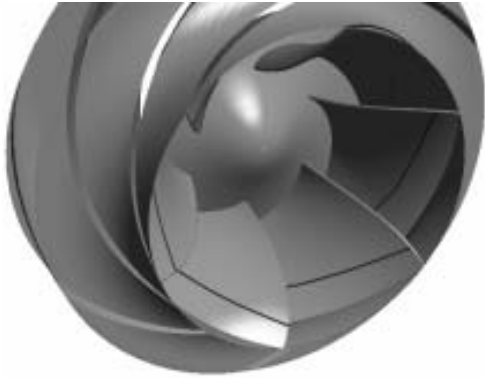


Fig. 2. Geometry of the 3D model of the pump shown in Fig. 1. The lines on the blades designate the streamline going through the region on the suction side of the blade most affected by cavitation erosion (compare to Fig. 1).

they reach a stronger collapse and higher forces generated by the bubble dynamics.

It should be remembered that the limiting value of the erosion driving forces  $EF$  at the boundary of the eroded region depends on the actual length of operation of the pump and the material properties of the blade surface. The value of the forces at the boundaries of the eroded region will depend on pumps and different numbers of operation cycles.

#### 4. Conclusions

The regions on the blades of the mixed-flow water pump impeller endangered by cavitation bubbles have been determined numerically. The comparison of the results with the eroded blades of the real pump showed that the quantities chosen as the approximate measures of the potential cavitation damage (the „erosion driving forces“) are able to delimit the area of erosion and to indicate the region of strongest damage.

In order to improve the simulation the length of operation and material fatigue must be included in the model and the numerical results must be compared with enough experimental data. The revised nucleation theory must be engaged in order to obtain the initial number of bubbles.

#### Acknowledgements

The authors wish to acknowledge the support of the Grant Agency of the Czech Republic (grant no. S2076003) and the Grant Agency of the Academy of Sciences of the Czech Republic (grant no. 101/04/P108).

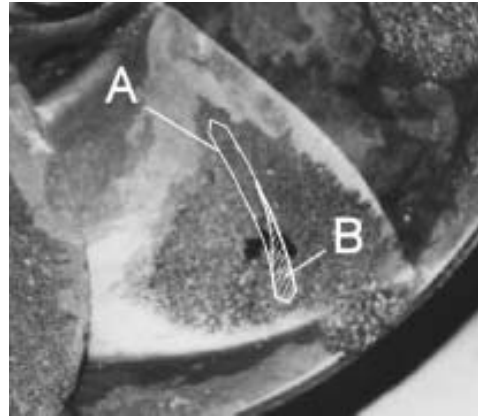


Fig. 3. Numerical results projected on the photograph of the pump blade: A – The region of the first collapses. B –  $\log_{10} |EF_1| > 6$ .

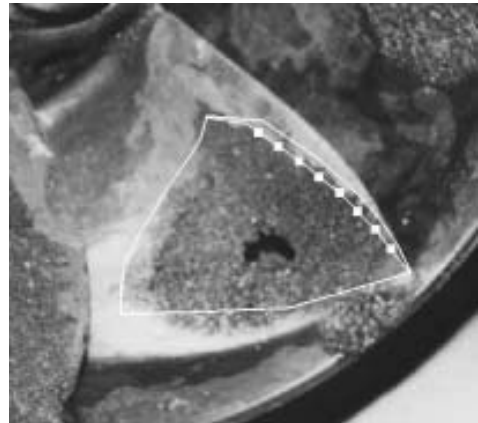


Fig. 4. Numerical results projected on the photo of the blade: Solid line –  $\log_{10} |EF_1| = 3$ . Line with squares –  $\log_{10} |EF_1| = 4$ .

#### References and Notes

- [1] Ch. E. Brennen, *Cavitation and Bubble Dynamics*, Oxford Univ. Press (1995).
- [2] F. Maršík, C.F. Delale, M. Sedlář, *Arch. of Thermodynamics*, **24**, 3 (2003).
- [3] P. Zima, F. Maršík, *J. Thermal Science*, **12**, 151 (2003).
- [4] M. Sedlář, *Int. J. Num. Meth. Fluids*, **16**, 963 (1993).
- [5] M. Sedlář, F. Maršík, P. Šafařík, *Proc. 5<sup>th</sup> ISAIF*, Gdansk, **1**, 237 (2001).
- [6] Y. Ch. Wang, *J. Fluids Eng.*, 881 (1999).
- [7] T. A. Waniewski, C. Hunter, Ch. E. Brennen, *Int. J. Multiphase Flow*, **27**, 1271 (2001).